J Mol Model (2013) 19:421–426
DOI 10.1007/s00894-012-1568-z

ORIGINAL PAPER

Structural phase transition of CdTe: an ab initio study

Sebahaddin Alptekin

Received: 11 April 2012 / Accepted: 9 August 2012 / Published online: 2 September 2012

Abstract A constant pressure ab initio MD technique and density functional theory with a generalized gradient approximation (GGA) was used to study the pressure-induced phase transition in zinc-blende CdTe. We found that CdTe undergoes a structural first-order phase transition to I$\bar{4}$m2 (binary β-tin) tetragonal structure in the constant pressure molecular dynamics simulation at 20 GPa. When the pressure was increased to 50 GPa, the phase of tetragonal structure converted to a new *Imm2* orthorhombic structure. These phase transformations were also calculated by using the enthalpy calculations. Transition phases, lattice parameters and bulk properties we attained are comparable with experimental and theoretical data.

Keywords Ab initio calculation · High pressure · Phase transformation · Semiconductor

Introduction

The pressure induced phase transitions have been studied by many scientists during the last decades [1]. Studies of the II–IV semiconductor CdTe have been occupied by uncertainties as to the structures of its high pressure phases. The enormous advances in the accuracy and efficiency of the first-principles electronic structure calculations have allowed detailed studies of the energetics and structural systematics of materials under high pressure. The pressure-induced structural phase transitions for Cd with S, Se and Te were first observed in optical studies around 3.5 GPa [2], electrical resistance at 10 GPa [3], and density measurements at 3.5 GPa [4]. CdTe is a II–IV group semiconductor compound under normal conditions, which has a cubic zinc-blende (ZB) structure. CdTe has been studied by high pressure x-ray diffraction with DAC and structural phase transition from ZB to rock-salt (RS) around 3.3 GPa at room temperature, from RS to β-tin phase at about 10.3 GPa and then to an orthorhombic structure with space group *Pmm*2 at about 12 GPa have been reported [5]. Recently, Nelmes and colleagues used angle-dispersive techniques and image-plate detectors and they found that, in fact, CdTe has two closely spaced transitions near 3.5 GPa: first ZB to cinnabar and then cinnabar to RS [6, 7]. Nelmes et al. [8] performed detailed angle-dispersive diffraction measurements on CdTe at around 28 GPa. They found that at 10 GPa the RS phase of CdTe transformed continuously into a *Cmcm* structure that remained stable until 28 GPa. They showed that two phases with β-tin type and with symmetry *Pmm2* are the same, and they supposed that the two phases belong to the *Cmcm* type. Structure of CdTe was studied by energy dispersive x-ray diffraction using synchroton radiation pressure and around 3.5 GPa, a transition first from ZB to cinnabar and then from cinnabar to RS was reported by Martínez-García et al. [9]. They obtained that the cinnabar phase appeared only in a very narrow pressure range and could be isolated only in the pressure decrease. The high-pressure phases of CdTe crystal was studied by Côté et al. [10]. Their results are comparable with experimental and theoretical results for lattice parameters and lattice constant ratios depending on pressure in *Cmcm* phase. Electrical properties and phase transition of CdTe under high pressure were studied by Chunyuan et al. [11] and it was obtained that at about 6.24 GPa, CdTe is a narrow band gap semiconductor.

In this paper, we carry out a constant pressure ab initio MD technique to study the pressure-induced phase transition in CdTe. We show that ZB CdTe undergoes I$\bar{4}$m2 (binary β-tin) tetragonal structure in the constant pressure molecular dynamics simulation and then into *Imm2* orthorhombic structure (Fig. 1). We also investigate the stability of ZB, I$\bar{4}$m2 and *Imm2* phases from energy–volume calculations.

S. Alptekin (✉)
Department of Physics, Çankırı Karatekin University,
Cankiri 18100, Turkey
e-mail: salptekin@karatekin.edu.tr

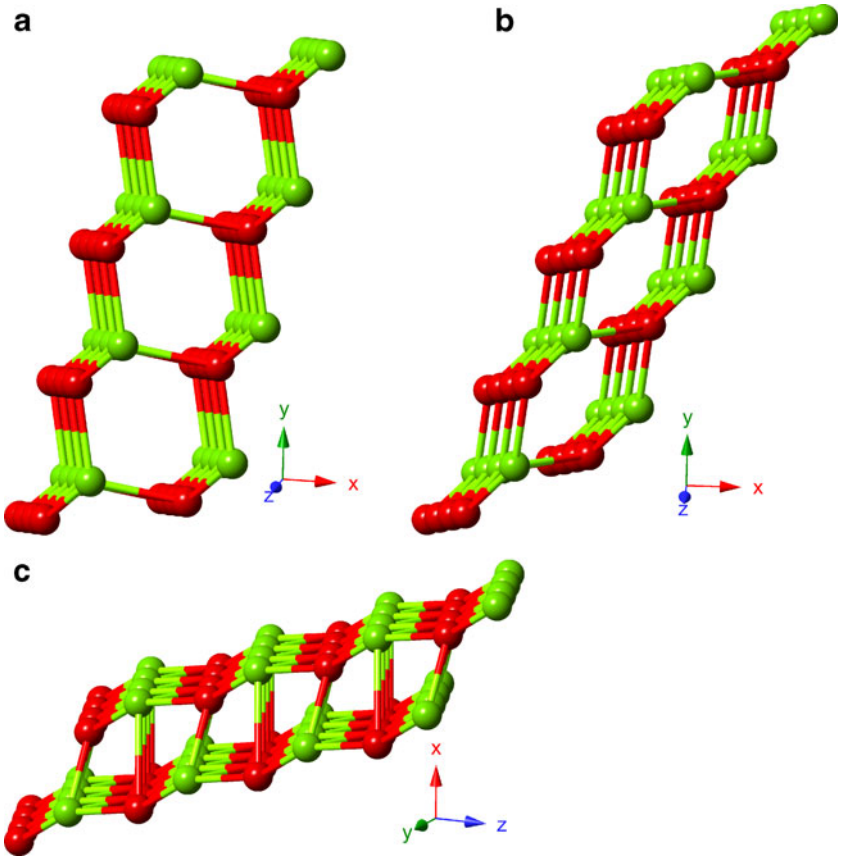

Fig. 1 Crystal structures of CdTe: **a** ZB phase at zero-pressure, **b** I$\bar{4}$m2 phase at 20 GPa and **c** *Imm2* phase at 50 GPa (the atoms Cd and Te have *red* and *green* colors, respectively)

Computational methods

All calculations were carried out using the SIESTA code [12]. We used the density functional theory (DFT) with the generalized gradient approximation (GGA) of Perdew-Burke and Ernzerhof (PBE) for the exchange-correlation energy [13]. The norm-conservative Troullier-Martins pseudopotentials [14] were employed for core electrons, and valent electrons were described with a split-valence double-ξ basis sets expanded with polarized functions. A uniform mesh with a plane wave cut-off of 150 Ry was used to represent the electron density, the local part of the pseudopotentials, and the Hartree and the exchange-correlation potential. The simulation cell consists of 64 atoms with periodic boundary conditions. We used Γ-point sampling for the supercell's Brillouin zone integration. The molecular dynamics (MD) simulations were performed using the NPH (constant number of atoms, constant pressure, and constant enthalpy) ensemble. The reason for choosing this ensemble is to remove the thermal fluctuation, which facilitates easier examination of the structure during the phase transformation. Pressure is applied via the method of Parrinello and Rahman [15] and structures were equilibrated with a period of 1000 time steps (each time step is one femto-second) at each applied pressure. The system was first equilibrated at zero pressure, and then pressure was gradually increased by an increment of 10.0 GPa. For each value of the applied pressure, the structure was allowed to relax and find its equilibrium volume and the lowest energy by optimizing its lattice vectors and atomic positions together until the stress tolerance was less than 0.5 GPa and the maximum atomic force was smaller than 0.01 eVÅ^{-1}. For the energy volume calculations, we only considered the unit cell for CdTe phases. The Brillouin zone integration was performed with an automatically generated 10×10×10 k-point mesh for the phases following the convention of Monkhorst and Pack [16]. In order to determine the symmetry of the high pressure phases formed in the simulations, we used the KPLOT program [17] that provides detailed information about the space group, the cell parameters and the atomic position of a given structure. For the symmetry analysis we used 0.2 Å, 4 ° and 0.7 Å tolerances for the bond length, bond angles and inter planar spacing, respectively.

Results

Enthalpy calculation

We studied calculations to find the equilibrium lattice parameters phases of CdTe. The unit cells of these structures are relaxed at zero pressure using the variable cell optimization technique and our result are given in Table 1. We

Table 1 The atomic fractional coordinates and equilibrium lattice parameters of the ZB, I$\bar{4}$m2 and *Imm2* phases

Structure	a (Å)	b (Å)	c (Å)	x	y	z
ZB	6.4266	6.4266	6.4266	Cd:0.000	0.000	0.000
				Te:0.250	0.250	0.250
I$\bar{4}$m2	5.2482	5.2482	3.1639	Cd:0.000	0.000	0.000
				Te:0.000	0.500	0.750
Imm2	5.0492	5.2145	2.7446	Cd:0.000	0.000	0.000
				Te: 0.000	0.500	0.8472

performed the total energy of these phases as a function of volume and their energy-volume relations were fit to the third-order Birch Murnaghan equation of states. The energy-volume curve of the structures is presented in Fig. 2 and as shown ZB structure has the lowest energy. On the other hand, to determine the most stable structure at finite pressure and temperature, the free energy $G=E_{tot}+PV-TS$ should be used. Our density functional calculations are basically completed at zero Kelvin temperature and entropic contributions can be ignored. Therefore, the enthalpy values, H=E+pV, including the pressure-volume effects are determined. This behavior is compatible with a phase transition between these structures, which is also clearly reflected in the enthalpy calculation.

Simple comparison of the static lattice enthalpies of ZB state, I$\bar{4}$m2 (binary β-tin) and the *Imm2* state determines the pressure of the transition between them. The crossing of three enthalpy curves indicates a pressure-induced phase transition between these phases. The computed enthalpy curves of the ZB, I$\bar{4}$m2 and *Imm2* phases are plotted as a function of pressure in Fig. 3. As can be seen from the figure, the enthalpy curves of the I$\bar{4}$m2 phase and *Imm2* phase have the same enthalpy and intersect with that of ZB phase at 4.8 GPa, indicating a first order phase transition between these phases. On the other hand, from the energy-volume data, we also calculate the bulk modulus of these phases. For the zinc-blende state, our bulk modulus is 53.2 GPa, which is relatively close to the theoretical values 46 GPa and 48.98 GPa [18, 19]. The bulk modulus can vary in a wide range according to the methodology of the study. The bulk modulus of the I$\bar{4}$m2 (binary β-tin) phase is calculated to be 70.7 GPa and the bulk modulus of the *Imm2* phase is calculated to be 75.7 GPa. In general, our results agree with the experimental and theoretical results.

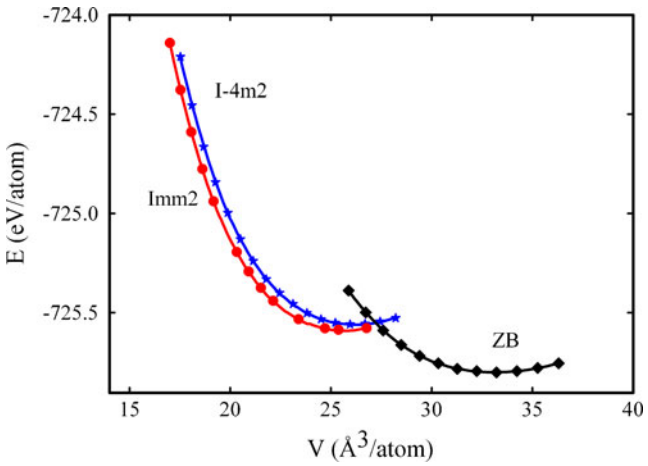

Fig. 2 The computed energies of ZB, I$\bar{4}$m2 and *Imm2* phase of CdTe phases as a function of volume

Parinello Rahman simulation

The pressure-volume relation of CdTe obtained through the constant pressure simulation can be seen in Fig. 4. As can be seen from the figure, the volume monotonically decreases with increasing pressure to 15 GPa. When the pressure is increased from 15 to 20 GPa the structural phase transition begins and volume shows a noticeable decrease, which is typical for a first order phase transition. The structural analysis brings out that zinc-blende CdTe converts into a I$\bar{4}$m2 (binary β-tin) structure. This tendency is indeed anticipated when some conditions in simulations are considered, namely, the use of ideal structure, the size of the simulated structure etc. Consequently, simulated systems have to cross a significant energy barrier to transform from one phase to another.

In this study, we are particularly interested in understanding the transformation mechanism to control structural phase transition. Therefore, as a next step, we studied the atomic movement during the phase transformation by

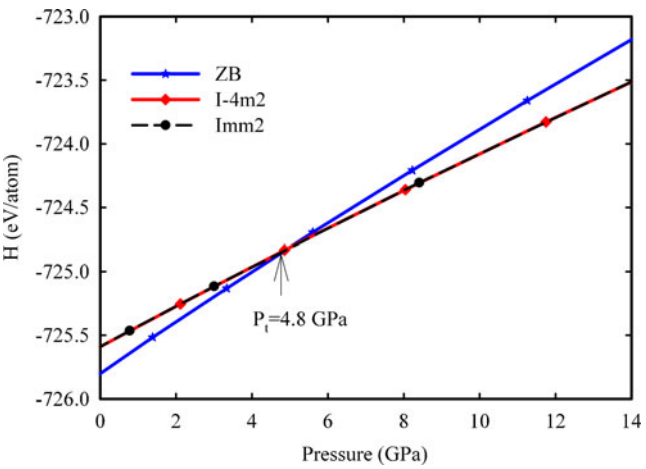

Fig. 3 Enthalpy *curves* of ZB, I$\bar{4}$m2 and *Imm2* phase of CdTe

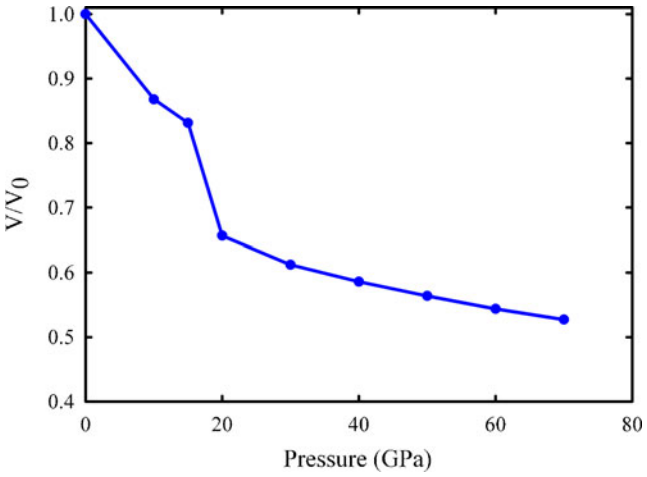

Fig. 4 Volume change as a function of hydrostatic pressure (the y axis contains normalized values)

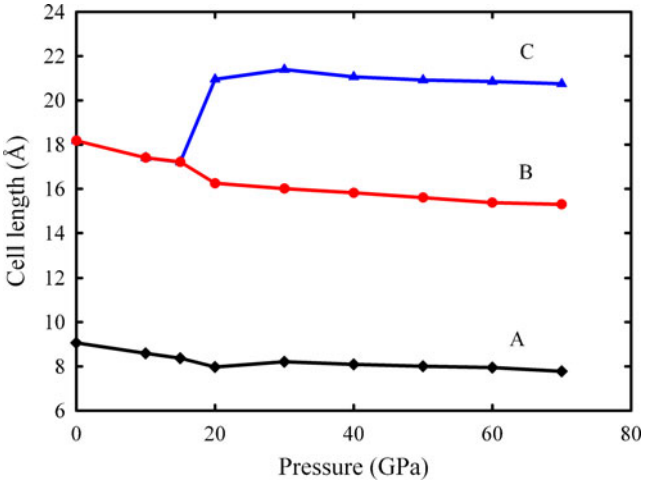

Fig. 6 Variation of simulation cell lengths as a function of applied pressure

analyzing the modification of the simulation cell and plot the simulation cell lengths and angles at 20 GPa as a function of minimization step in Fig. 5. The simulation cell vectors A, B, and C are originally along the [100], [010] and [001] directions, respectively. The magnitude of these vectors is plotted in the figure. As clearly seen from the figure, the transformation mechanism from ZB to I$\bar{4}$m2 (binary β-tin) structure in CdTe is straightforward and there is no change in |A|, a noticeable increase in |B| and a noticeable decrease in |C|; and the simulation cell angles α (between B and C lattice vectors) and γ (between A and B lattice vectors) decrease from 60° to about 49° while β (between A and C lattice vectors) increases from 60° to about 81° simultaneously, resulting in a I$\bar{4}$m2 (binary β-tin) modification of the simulation cell during the phase transformation. The structural analysis using the KPLOT program [17] indicates that this state has a tetragonal structure within I$\bar{4}$m2 (binary β-tin) symmetry. The lattice constants of I$\bar{4}$m2 (binary β-tin) phase are a=3.221 Å, b=6.235 Å and c=6.634 Å and the lattice constants of *Imm2* phase are a=

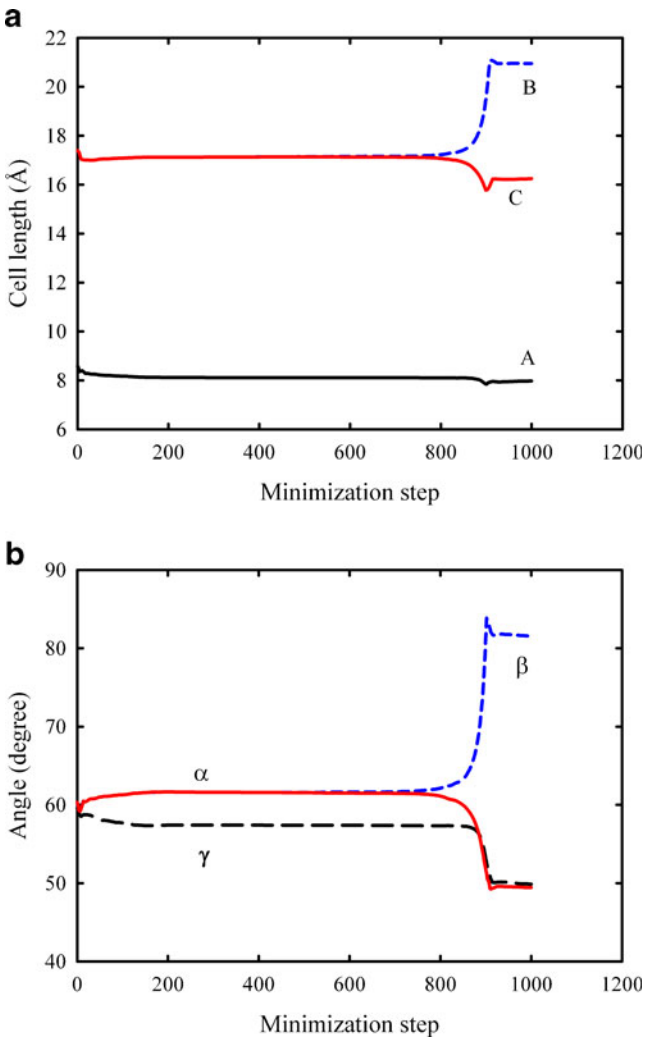

Fig. 5 Change the simulation cell lengths and angels as a function of minimization step at 20 GPa

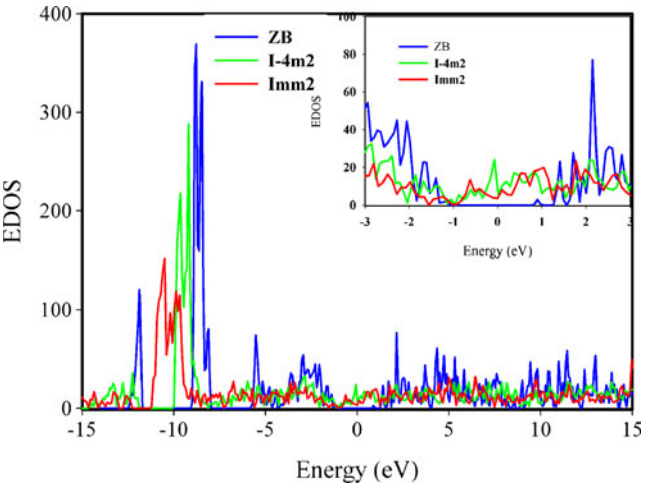

Fig. 7 Calculated electronic density of states (EDOS) for CdTe at 0 GPa (ZB phase), 20 GPa (I$\bar{4}$m2) and 50 GPa (*Imm2*)

5.0492 Å, b=5.2145 Å and c=2.7446 Å. When I$\bar{4}$m2 (binary β-tin) structures and *Imm2* are compared, at the beginning, ZB phase is four-fold coordinated, the resultant I$\bar{4}$m2 (binary β-tin) phase is four-fold coordinated and *Imm2* phase is six-fold coordinated. Therefore, the transformation pathway of ZB-CdTe in the simulation is based on both tetragonal I$\bar{4}$m2 and orthorhombic *Imm2* intermediate state. In Fig. 6, variation of simulation cell lengths as a function of pressure is also given. We also dealt with that high pressure phases of CdTe are semiconductor or semimetal. We find that band gap of ZB- CdTe is 2.1 eV at 0 GPa and experimental value is between 1.60 and 2.55 eV [20]. We also investigated that tetragonal I$\bar{4}$m2 at 20 GPa and orthorhombic *Imm2* at 50 GPa. The electron density of states (EDOS) of high pressure phases and ZB are pictured in Fig. 7. It is seen that there is no electron density of states between −1 eV and 1 eV at 0 GPa. Therefore, ZB phase of CdTe is semiconductor and since there is no such interval for the other phases we find that both high-pressure phases of CdTe are semimetals in Fig. 7.

Discussion

Using a constant pressure ab initio technic, we have studied the pressure-induced phase transition in CdTe. We found that new phases of ZB-CdTe can transform from one phase to another by passing through various closely related paths during the transformation. In other words, the transformation mechanism might follow various paths or involve several intermediate states. Transition paths followed under hydrostatic pressure are ZB→I$\bar{4}$m2→*Imm2* and the same transition paths for GaAs are observed by Durandurdu [21]. On the other hand, transitions from zinc-blende CdTe to rock-salt, from rock-salt to β-tin phase and then to an orthorhombic structure with space group *Pmm*2 are reported by Hu [5]. In an experimental study, transitions from zinc-blende to cinnabar and then to NaCl-type phase were observed by Sowa [22]. And in some others, some structures such as Wurtzite (WZ) or zinc-blende (CdSe, BeO) were transformed into RS structure [23, 24]. Therefore, we expect to see analogous transformation mechanisms and probably the formation of β-tin and *Imm2* or closely related structures in other diamond and ZB structured materials. In a previous study, Nelmes et al. [8] found that NaCl phase of CdTe transformed into *Cmcm* structure. They showed that two phases with β-tin type symmetry and with *Pmm2* type symmetry are the same, and they supposed that the two phases belong to the *Cmcm* type. In our previous study [25], we studied ZnTe under hydrostatic pressure using an ab initio constant pressure MD technique and found a phase transition from WZ structure to a *Cmcm* structure. In our current study, we found the lattice parameters for ZB phase. The calculated lattice parameter is a=6.426 Å for the ZB phase in agreement with the experimental value a=6.480 Å, in addition, the calculated bulk modulus is 53.2 GPa and experimental value for the ZB phase is calculated to be 44.5 GPa [20]. In general, our results showed the agreement for ZB phase with the experimental and theoretical results.

Conclusions

We have used an ab initio constant pressure MD technique within a generalized gradient approximation (GGA) to study the pressure-induced phase transition in CdTe. The ZB structure transforms into a tetragonal state with space group I$\bar{4}$m2 at 20 GPa and this phase is still four-fold coordinated. With an increase in pressure a continuous phase change to an orthorhombic six-fold coordinated Imm2 structure occurs at 50 GPa. In addition, we obtain enthalpy calculations from the energy-volume for three structural phases of CdTe. The electron density of states (EDOS) of high pressure phases and ZB are calculated. Our calculated transition phase, lattice parameters and bulk modulus are in agreement with experimental and theoretical data.

Acknowledgments We are grateful to Dr. Murat Durandurdu for his help. We are grateful to the SIESTA group for making their code publicly available.

References

1. Mujica A, Rubio A, Muñoz A, Needs RJ (2003) Rev Mod Phys 75:863–912
2. Edwards AL, Drickamer HG (1961) Phys Rev B 122:1149–1157
3. Samara GA, Drickamer HG (1962) J Phys Chem Solids 23:457–461
4. Jayaraman A, Klement W Jr, Kennedy GC (1963) Phys Rev B 130:2277–2283
5. Hu JZ (1987) Solid State Comm 63:471–474
6. Nelmes RJ, McMahon MI, Wright NG, Allan DR (1993) Phys Rev B 48:1314–1317
7. McMahon MI, Nelmes RJ, Wright NG, Allan DR (1993) Phys Rev B 48:16246–16251
8. Nelmes RJ, McMahon MI, Wright NG, Allan DR (1995) Phys Rev B 51:15723–15731
9. Martínez-García D, Le Godec Y, Mézouar M, Syfosse, Itié JP, Besson JM (1999) Phys Stat Sol (b) 211:461–467
10. Côté M, Zakharov O, Rubio A, Cohen ML (1997) Phys Rev B 55:13025–13031
11. He C, Gao CX, Liu BG, Li M, Huang XW, Hao AM, Yu CL, Zhang DM, Wang Y, Liu HW, Ma YZ, Zou GT (2007) J Phys Condens Matter 19(8):425223
12. Ordejòn P, Artacho E, Soler JM (1996) Phys Rev B 53:10441–10444
13. Perdew JP, Burke K, Ernzerhof M (1996) Phys Rev Lett 77:3865–3868

14. Troullier N, Martins JM (1991) Phys Rev B 43:1993–2006
15. Parrinello M, Rahman A (1980) Phys Rev Lett 45:1196–1199
16. Monkhorst HJ, Pack JD (1976) Phys Rev B 13:5188–5192
17. Hundt R, Schön JC, Hannemann A, Jansen M (1999) J Appl Crystallogr 32:413–416
18. Yang JH, Chen S, Yin WJ, Gong XG, Walsh A, Wei SH (2009) Phys Rev B 79(7):245202
19. Deligoz E, Colakoglu K, Ciftci Y (2006) Physica B 373:124–130
20. Madelung O, Schulz M, Weiss H, Landolt-Börstein (eds) (1982) Numerical data and functional relationships in science and technology, vol 17. Springer, Berlin
21. Durandurdu M (2006) J Phys Condens Matter 18:4887–4894
22. Sowa H (2005) J Appl Cryst 38:537–543
23. Durandurdu M (2010) Chem Phys 369:55–58
24. Alptekin S, Durandurdu M (2009) Solid State Commun 149:345–348
25. Alptekin S (2011) J Mol Model 18:1167–1172